Defence Science Journal, Vol. 73, No. 4, July 2023, pp. 487-495, DOI : 10.14429/dsj.73.18174

Delamination Buckling of Composite Conical Shells Under External Pressure

A. Nagendranath[#,*], Sanjay A. Khalane[#], R.K. Gupta[#] and C. Lakshmana Rao[$]

[#]*DRDO-Advanced Systems Laboratory, Hyderabad - 500 058, India*

[$]*Department of Applied Mechanics, IIT Madras, Chennai - 600 036, India*

[*]*E-mail: nagendranatha.asl@gov.in*

ABSTRACT

Airframe construction in conical form is the most desired shape of flight hardware due to their low drag profile and are located at the fore-end region of flight vehicles encountering high drag loads. Owing to their tailoring capability, materials with orthotropic mechanical properties are preferred choice. Delamination defects formed in them while manufacturing or when subjected to loads would unfavorably influence the mechanical performance of the orthotropic airframe. In the current work, FE simulation of delamination which is embedded in orthotropic cone shaped shells under external pressure load is performed as per the method cited in published literature. A layer wise element based on shell theory has been used and the effect of delamination size and its through the thickness position on the mechanical performance of the cone shaped shell is investigated. Circumferential and rectangular shapes of defects have been simulated. The investigation is performed for metal and composite materials with 3 types of stacking sequences generally used in practical designs. Verification of the procedure is carried out by equating with the procedure cited in published studies on shells of thin orthotropic cylinders. The eigen value of the first mode is taken as the critical buckling factor under external pressure. The buckling factor of the delaminated cone is normalized with the buckling factor of the ideal cone. The normalized buckling factor is showed graphically with the normalised defect size. Global, as well as local buckling and also symmetric as well as asymmetric buckling shapes, are observed in the results of the simulation. Shift from global mode to local mode of buckling is also observed in certain cases. Drastic reduction in buckling capability with the local mode is observed when the defect location is close to the surface and more prominent for an outer surface case.

Keywords: Composite shells; Delamination; Buckling; Conical shells; External pressure

NOMENCLATURE

[A] - Extensional stiffness matrix
N_6 - Shear force resultant in x_1 to x_2 direction
[B] - Bending-extensional coupling stiffener matrix
$\widehat{N}$ - Axial compressive load (+ in compression)
[D] - Bending stiffness matrix
Q_1 - Transverse shear force in x_1 direction
d1 - Lower diameter of the cone
Q_2 - Transverse shear force in x_2 direction
d2 - Higher diameter of the cone
$\bar{Q}$ - Transformed stiffness matrix
E_L - Young's modulus in the longitudinal direction
t - Location of defect/delamination from the inner surface
E_T - Young's modulus in the transverse direction
T - Total thickness of the shell
G_{LT} - In plane shear modulus
u_0 - Translation of mid surface in x_1 direction
υ - Poisson's ratio
h - Ratio: location of delamination from inner surface / total thickness
v_0 - Translation of mid surface in x_2 direction
K_S - Shear correction factor
w_0 - Translation of mid surface in x_3 direction
L - Length of the cone
x_1 - Meridional direction
Ld - Length of delamination
x_2 - Circumferential direction
[M] - Column matrix of M_1, M_2 & M_6
x_3 - Normal direction
M_1 - Moment resultant in x_1 direction
α - Width of delamination in degree
M_2 - Moment resultant in x_2 direction
ϕ - Rotation normal to reference surface
M_6 - Moment resultant in x_1 to x_2 direction
η (eta) - Element natural coordinate in x_1 direction
[N] - Column matrix of N_1, N_2 & N_6
ξ (xi) - Element natural coordinate in x_2 direction
N_1 - Force resultant in x_1 direction
ψ (psi) - Lagrange interpolation function
N_2 - Force resultant in x_2 direction
ζ (zeta) - Natural coordinate in x_3 direction

Received : 13 May 2022, Revised : 05 April 2023
Accepted : 13 April 2023, Online published : 11 July 2023

1. INTRODUCTION

Composite materials are preferred in the design of flight vehicles because of their high specific strength and specific modulus. Thin shell construction constitutes the major geometries of flight configurations. Conical shells are the most appropriate aerospace structures owing to their smooth shape that offer less drag and located in the leading region of flight structures that undergo sever loads.

In orthotropic thin shells, flaws of the nature of delamination / de-bond generate during manufacturing or when subjected to loads. These flaws would decrease the stiffness due to the absence of through the thickness reinforcement. The residual stiffness and strength depend on the geometry and through the thickness position of the flaw.

Aerodynamic load on the aerospace structure during flight condition arise from external pressure, causing compressive nature of stress, in a biaxial direction. Compressive stress initiates failure of the cone not only by stress measures but also through geometric buckling. The instability can occur before failure by stress if the shell is insufficiently stiff. The existence of defects additionally reduces the shell stiffness and drastically lowers the buckling factor. Laminate separation at the zone of delamination contributes to the reduction.

Sufficient studies are available in the literature on various techniques and methods for the evaluation of residual strength and stiffness of laminated plates. Circular cylindrical laminated shells with de-bond and de-laminations are also studied exhaustively[1-9]. As discussed, conical laminated composite shells form the primary airframe structures in advanced launch vehicles and missiles. Very meager literature is available on the de-lamination aspects of the conical shell. Authors have studied this gap in research which is much needed for today's practical use of laminated conical shells with advanced composite materials.

In the present study, numerical simulation is carried out to evaluate the buckling capability of composite conical shells with embedded delamination. Carbon fiber-based epoxy composite material system has been chosen for simulations on two types of delamination, viz. rectangular delamination and circumferential delamination. The effect of depth-wise, circumferential and longitudinal location and size of defect are thoroughly investigated.

2. LITERATURE REVIEW

The existence of delamination will lessen the load-bearing ability of thin shells made of orthotropic materials[1]. Many studies have been performed by researchers on the implication of delamination on structures. The vast amount of the published literature present the studies on delamination in beams and plates. The available literature on shells and curved panels considering buckling behavior in the presence of delamination is limited. The most similar research effort in the present area of work is published by Simitses[2-3] and Tafreshi[4-5].

Analytical formulation from membrane theory of shell with subsequent numerical solution has been performed by Simitses[2] on delamination buckling of very long cylindrical shells under external pressure. The investigation has been for isotropic materials with longitudinal delamination over the entire length with simply supported as well as clamped boundary conditions. Auxiliary conditions involving kinematic continuity and local equilibrium conditions have been considered along the common boundaries between the perfect zone and the delaminated zone. The effect of size and through-the-thickness position of delamination is studied. It is assumed that the implication of the through-the-thickness position is symmetric about the mid-thickness of the shell. Critical buckling loads for the different angular sizes of delamination have been presented for cylindrical shells and quarter as well as half panels. The larger the delamination size, the lower the buckling capability is the observation. When the through-the-thickness position is close to the surface, the observation is a local buckling mode and has the lowest critical load for a delamination size. Orthotropic Graphite / Epoxy material with stacking sequence $[90°/0°/90°]_{10T}$ has been considered by Simitses[3] in the study of delamination buckling of cylindrical laminates and reported similar aforesaid observations. In both works, there is a likelihood of delaminated layers penetrating each other and altering the observed results as the feature that prevents penetration is not incorporated in the mathematical model.

A finite element-based study on delamination buckling of cylindrical shells under external pressure, utilizing the contact element/gap element to avoid interpenetration of delaminated layers has been carried out by Tafreshi[4]. A combination of a single layer and a double layer of shell elements has been employed which reduced the computation time as compared to 3D elements. The effect of material properties and stacking sequence is studied along with the size and through-the-thickness position. A raise in buckling load is observed due to incorporation of contact elements in the finite element model. The applied boundary conditions would result in a shell with a uniaxial state of stress whereas the shell would be in a biaxial state of stress. The rectangular delamination simulated spans from end to end and would be affected by the end boundary conditions. This geometry would not simulate embedded delamination which is of present attention.

Experimental investigations and corresponding numerical simulations of filament wound composite tubes under axial compression have been made by Jose Humberto S.[6], *et al.* The investigation involved testing tubes till buckling failure with various helical angles and thicknesses. The study demonstrated the adequacy of linear finite element analysis for thin tubes and helical plies of unique angles which failed by buckling. Thicker and helical plies of multiple angles needed nonlinear simulation involving progressive damage based on the Continuum Damage Model for better correlation as the failure of tubes is by material damage. Delamination is not included either in the numerical simulation or testing.

For underwater application which is another area of weight-sensitive application, large-sized pipes made of composites are subjected to bending loads due to support conditions. Results of collective experimental and numerical analysis of large-scale filament wound composite pipes under four-point bending are published by Zhenyu Huang[7], *et al.* A layered shell with multiple angles failed at higher flexural strength than with layered shell with a unique angle. Delamination is the failure mode observed rather than as a source of failure.

Numerical simulation of buckling and post-buckling of curved composite panels subjected to axial load in compression has been carried out by Behnam Ameri[8], *et al.* Curved panels of various included angles have been analyzed through the width delamination located at the mid thickness and near the surface. This parametric study involved fiber angle and stacking sequence concluding that the buckling load is considerably affected by near-surface delamination.

Investigation of transverse deflection of conical roof structures made of composites with local supports under various delamination sizes is performed by Kamalika Das[9], *et al.* The transverse deflection is reported to be directly proportional to the area of delamination. For a typical delamination size, the deflection is reduced by a greater number of supports and a greater number of plies. Symmetric cross-ply and antisymmetric angle plies have demonstrated lower transverse deflections among various stacking sequences studied.

Most of the testified work is on thin cylinders with cross-ply stacking sequence. Inadequate literature is existing on cones. Available classical work[10] is based on the equivalent cylinder with fore-end geometric details, the outcome of which would be a conservative design. For a weight-sensitive area of application like aerospace, it is not satisfactory. Large-sized orthotropic cones are realized by filament winding technique and at any station in the longitudinal direction, the stacking order is angle-ply of varying angles. Therefore, the study on conical shells having angle-ply stacking order with angle varying in longitudinal direction would be of direct applicability.

The study is also performed for isotropic material (Aluminum) and cross-ply sequence. Two variants of stacking orders of cross-ply arrangement are simulated. One cross-ply sequence is (0^0, 90^0, 0^0)s, designated as cross-ply0 and the other cross-ply sequence is (90^0, 0^0, 90^0)s, designated as cross-ply90.

3. METHODOLOGY

The geometric details of the carbon epoxy cone having 8.5^0 half-cone angle is in Fig. 1 along with two types of delamination rectangular and circumferential. Studies have been carried out for a load of external pressure with delamination present at $1/8^{th}$, $1/4^{th}$, 1/2, $3/4^{th}$, and $7/8^{th}$ shell thickness, represented as delamination thickness: h of 0.125, 0.25, 0.5, 0.75 and 0.875 respectively (non-dimensional term; position of delamination/total thickness). The presence of delamination is referred from the internal surface of the cone. The delamination is supposed to be present at mid of the cone and grows in equal increments to both sides in the longitudinal direction in the case of circumferential delamination. For the rectangular case, delamination is supposed to be present at mid of the cone and progress in the circumferential direction. For the angle-ply case, the stacking order is $\pm \theta^0$ with variation in the length direction. For the geodesic winding, at the middle of the cone, θ is 35^0, and variation is calculated using Clairaut's relation.

4. FINITE ELEMENT MODEL DETAILS

The cone is meshed with element based on shell theory using SHELL 281[11], 8 noded element of Ansys, a general-purpose FEA software. The element behavior is based on the First-order Shear Deformation shell Theory (FSDT). The relevant equations for degrees of freedom, strain displacement relations, constitutive relations, and governing differential equations are provided in Appendix.

The integral region in the FE geometry is discretized with element size of 5 mm. The delaminated region and the transition region are discretized with an element size of 2 mm. The integral region in the FE geometry is discretized with one element in thickness direction. The delaminated region is meshed with two elements in thickness direction and contact feature linking the two elements for force transmission and interpenetration stoppage. These linking elements exhibit compression-only behavior which provides resistance when compressive force transmits through them and does not provide resistance when tensile load transfers separates them; therefore, a contact based non-linearity is present. The intermediate zone is discretized with two elements and a multi-point constraint joining the two elements. Section offset feature has been used to preserve the consistency of the middle surface in the longitudinal direction of the conical shell, which is plotted in Fig. 2.

A mesh convergence study is carried out to ascertain the adequacy of discretization. Although the regular buckling analysis is not highly sensitive to element size, because of the presence of contact elements which introduces nonlinearity the mesh convergence is evaluated. The evaluation is performed for an isotropic conical shell with circumferential delamination of L/3 for a delamination thickness of 0.5. The mesh size is altered in delamination zone only and the results of the evaluation are mentioned in Table 1. As the difference in result between medium and fine meshes is 2 %, in view of the solution times for multiple simulations, medium mesh is preferred.

Table 1. Convergence study result

	Coarse	Medium	Fine
Element size, mm	4	2	1
% difference in buckling factor	4.2		2.0

The finite element model which is used in this study involves 30256 elements and 57096 nodes. External pressure is applied as surface load and axial load consistent with longitudinal stress is applied on the smaller end of the cone, simulating a biaxial stress state. At the fore-end of the cone, degrees of freedom other than longitudinal translation are constrained. Rear end of the conical shell is constrained in all directions representing clamped condition. A parametric script using Ansys Parametric Design Language[11] has been developed to automate the change in delamination size and contact area size. The material and geometric details of the conical shell considered in this study are as mentioned in Table 2.

Table 2. Geometry and material data

Geometric details of conical shell	**Length, L, mm**	**Lower diameter, d1, mm**		**Thickness, T, mm**
	320	96		4
Lamina properties	E_L, GPa	E_T, GPa	G_{LT}, GPa	υ
	115	6	4	0.25

5. VALIDATION STUDY

Corroboration of the current procedure has been performed by carrying out a simulation of an orthotropic thin cylinder of graphite-epoxy (stacking sequence: $[90°/0°/90°]_{10}$) with both ends simply supported[9] under external pressure, matching with the simulation by Tafreshi[4]. Rectangular delamination of width (a) extended over entire length and geometric features L to R = 6, R to t = 100 & h = 1/2 is taken for comparison. Buckling factors are standardized with the buckling factor of the perfect cylindrical shell. A comparison of normalized critical loads with that of reference data is shown in Fig. 3. As there is a good agreement, the methodology is validated and the study can be extended to conical geometry. A peak error of 4 % is noted, the possible causes being discretization difference and time increments that are not stated in the mentioned publication.

6. RESULTS AND DISCUSSION

In this section, results for the conical shell under external pressure are discussed. The eigen value buckling factor is considered as the critical external pressure. The first mode is considered irrespective of the buckled shape because large amount of distortion of the conical shell would increase the drag on the vehicle which is undesirable. Combinations of global & local and symmetric & asymmetric mode shapes are noticed in the outcome of the study which are shown in Fig. 4. Global buckling is noticed majorly for depths of 0.25, 0.5, and 0.75.

The critical external pressure of cone with defect is standardized with the critical external pressure of the ideal cone. The normalized critical pressure vs. the normalized length of delamination is presented in graph form in Fig. 5 – Fig. 8 for isotropic, angle-ply, cross-ply0, and cross-ply90 respectively for various depths of delamination.

For the isotropic case (Fig. 5), at depths of 0.125 & 0.25, for circumferential defect, global symmetric modes are observed and for rectangular defect, global asymmetric modes are observed. Mode shape remained the same with a reduction in buckling factor as the defect length is increased. At depth of 0.5, for circumferential defect, a global symmetric mode is observed till defect length of 0.19 and a local symmetric mode is observed beyond this defect length, hence a change in the slope of the curve is seen. For rectangular defects, a global symmetric mode is observed till the defect width of 45^0 and a global asymmetric mode is observed. There is no effect of defect width on buckling load factor beyond defect width of 225^0. At depth of 0.75, for circumferential as well as rectangular defects, the buckling mode is global symmetric and located beyond the defect zone. Hence defect length and width have no implication and a flat curve is seen. At a depth of 0.875, local modes have been observed with a drastic reduction in buckling capability for both types of defects.

For the angle-ply case (Fig. 6), a similar tendency as that of the isotropic case has been observed with a minor change in values of defect length and width, beyond which the buckling capability is independent of defect size. For rectangular defects, the curves of 0.125 and 0.875 are identical, unlike the isotropic case.

Table 3. Summary of simulation results

Legend: G – Global, L – Local, S – Symmetric, A – Asymmetric

Depth of ↓ delamination		Isotropic	Angle-ply	Cross-ply0	Cross-ply90
0.125	Circum.	G & S	G & S	G & S till defect length 0.05 and L & S beyond	G & S till defect length 0.05 and L & S beyond
	Rectangular	G & A	G & A	G & A till defect width 45^0 and L & A beyond. No effect of defect width beyond 45^0	G & A till defect width 45^0 and L & A beyond. No effect of defect Width beyond 45^0
0.25	Circum.	G & S	G & S	G & S	G & S
	Rectangular	G & A	G & A. No effect of defect width beyond 225^0	G & A	G & A
0.5	Circum.	G & S till defect length 0.19 and L & S beyond	G & S till defect length 0.2 and L & S beyond	G & S till defect length 0.2 and L & S beyond	G & S till defect length 0.18 and L & S beyond
	Rectangular	G & S till defect width 45^0 and G & A beyond	G & S till defect width 45^0 and G & A beyond. No effect of defect width beyond 180^0	G & A. No effect of defect width beyond 180^0	G & A. No effect of defect width beyond 225^0
0.75	Circum.	G & S. beyond defect zone	G & S beyond defect zone	L & S. No effect of defect length beyond 0.125	L & S. No effect of defect length beyond 0.1
	Rectangular	G & S. beyond defect zone	G & S beyond defect zone	L & A. No effect of defect width beyond 45^0.	L & A. No effect of defect width beyond 45^0.
0.875	Circum.	L & S	G & S. identical to 0.125	L & S. No effect of defect length beyond 0.05	L & S. No effect of defect length beyond 0.025
	Rectangular	L & A	G & A. identical to 0.125	L & A. No effect of defect width beyond 10^0.	L & A. No effect of defect width beyond 5^0.

For cross-ply0 and cross-ply90 case (Fig. 7 & Fig. 8), for circumferential defect, global symmetric modes are observed at depths of 0.125, 0.25 & 0.5 and local symmetric modes at depths of 0.75 & 0.875. For rectangular defects, asymmetric modes are observed which are global at depths of 0.125, 0.25 & 0.5, and local at depths of 0.75 & 0.875. When there is a shift from global mode to local mode, a change in the slope of the curve is seen and a flat curve is seen when the effect of defect size is negligible on the buckling capability. The observations are summarized into Table 3.

This simulation data also can be observed for various delamination depths, while comparing stacking sequences of angle-ply, cross-ply0, and cross-ply90. For delamination depth of 0.125, angle-ply exhibits a comparatively greater buckling factor under delamination. At depths of 0.25 & 0.5, there is the minimum influence of stacking sequence. At depth of 0.75, there is a minimum influence of delamination size on angle-ply as the buckling modes are located outside the delamination zone. At depth of 0.875, a drastic reduction of buckling capability is observed for all three stacking sequences.

7. CONCLUSION

A detailed study for assessing the residual capability of cones with embedded delamination under external pressure is carried out. A corroboration using this procedure is performed for thin cylinders and validated with the available literature. A fair comparison is observed. Subsequently, the procedure is extended to conical shells with isotropic material, angle-ply, and two variants of cross-ply.

The localized modes are noticed for delamination depths of 0.125 and 0.875 when the defect is located close to the surface. Buckling mode shapes are symmetric in the case of the circumferential defect and asymmetric modes in the case of the rectangular defect (other than 360^0). A regular pattern of a drastic reduction in buckling load as the defect location is close to the surface and more distinct when it is located close to the outer surface is observed.

The bifurcation buckling effects represent the upper limits of the assessments because of the perfect linear elastic shell and stable defect idealized in the present work. The finite element model will be augmented with geometric nonlinearity in future studies.

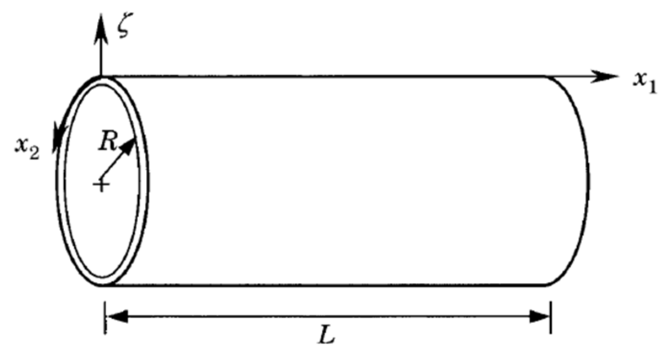

Figure A. Laminated shell geometry and coordinate system[12].

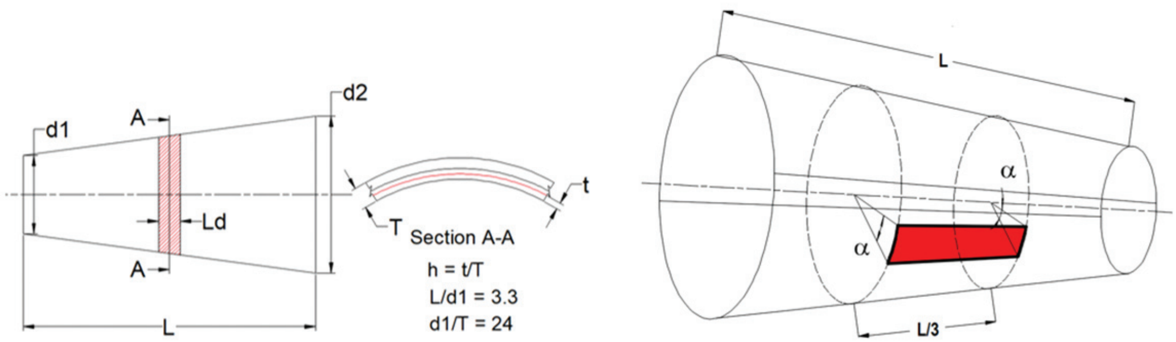

(i) Circumferential delamination

(ii) Rectangular delamination

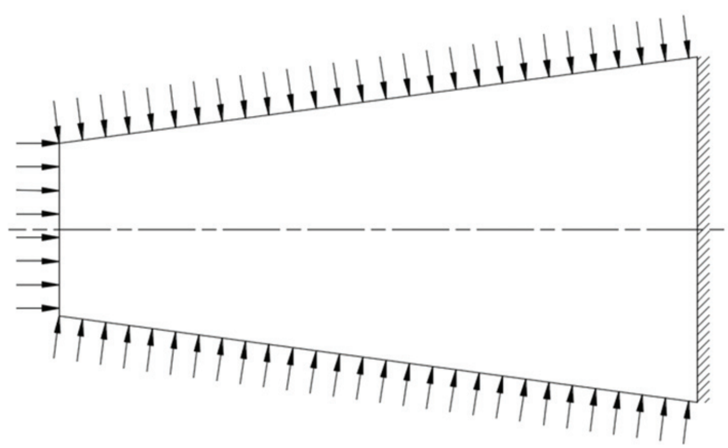

Figure 1. Conical shell with delamination under external pressure.

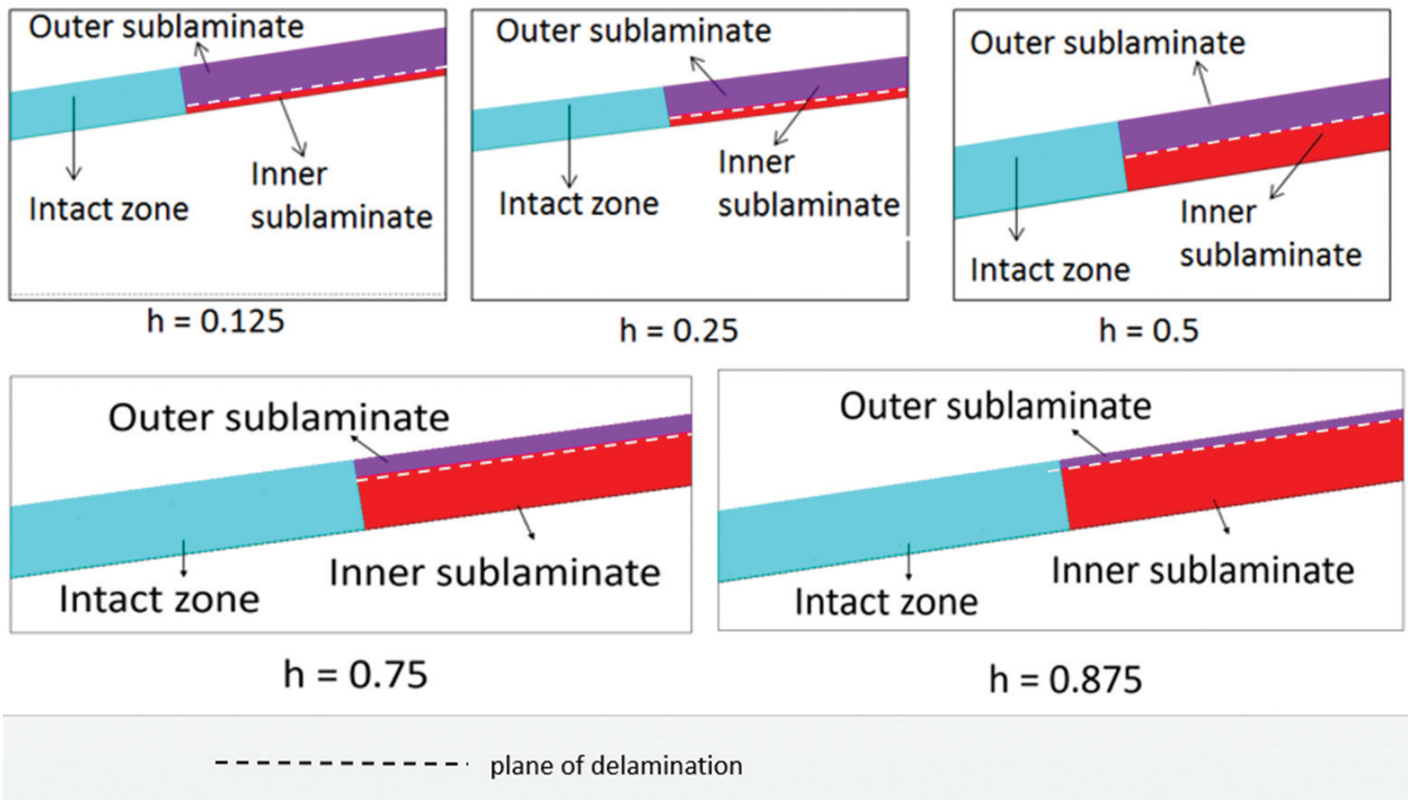

Figure 2. Section-offset for continuity of middle surface for different ratios of sub-laminates.

- Translational degree of freedom of mid surface in x_1 direction, u_0 is given by

$$u_0(x,y,t) \approx \sum_{j=1}^{m} u_j^e(t)\psi_j^e(x,y) \qquad (1)$$

where, ψ is the displacement interpolation function, expressed in terms of element natural coordinates given as follows for an 8 node quadratic element.

$$\begin{Bmatrix} \psi_1^e \\ \psi_2^e \\ \psi_3^e \\ \psi_4^e \\ \psi_5^e \\ \psi_6^e \\ \psi_7^e \\ \psi_8^e \end{Bmatrix} = \frac{1}{4}\begin{Bmatrix} (1-\xi)(1-\eta)(-\xi-\eta-1) \\ (1+\xi)(1-\eta)(\xi-\eta-1) \\ (1+\xi)(1+\eta)(\xi+\eta-1) \\ (1-\xi)(1+\eta)(-\xi+\eta-1) \\ 2(1-\xi^2)(1-\eta) \\ 2(1+\xi)(1-\eta^2) \\ 2(1-\xi^2)(1+\eta) \\ 2(1-\xi)(1-\eta^2) \end{Bmatrix} \qquad (2)$$

- Strain displacement relations as per first order shear deformation shell theory are given as follows.

$$\varepsilon_i = \varepsilon_i^0 + \zeta\varepsilon_i^1 \quad \textit{for i = 1, 2, 6}$$

$$\varepsilon_i = \varepsilon_i^0 \ \textit{for i = 4,5} \qquad (3)$$

$$\varepsilon_1^0 = \frac{\partial u_0}{\partial x_1},\ \varepsilon_1^1 = \frac{\partial \phi_1}{\partial x_1}$$

$$\varepsilon_2^0 = \frac{\partial v_0}{\partial x_2} + \frac{w_0}{R},\ \varepsilon_2^1 = \frac{\partial \phi_2}{\partial x_2}$$

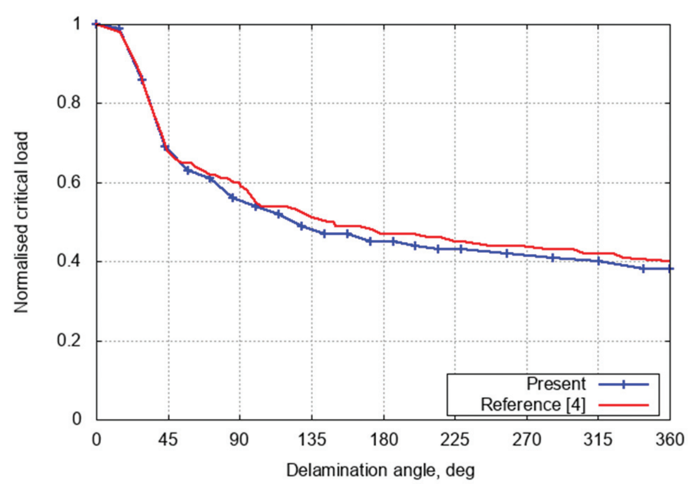

Figure 3. Critical buckling pressure vs effect of delamination width evaluation for cylindrical shell with delamination extended over the entire length, at a depth of 0.5 with contact elements.

$$\varepsilon_6^0 = \frac{\partial v_0}{\partial x_2} + \frac{\partial u_0}{\partial x_2},\ \varepsilon_6^1 = \frac{\partial \phi_2}{\partial x_1} + \frac{\partial \phi_1}{\partial x_2}$$

$$\varepsilon_4^0 = \phi_2 + \frac{\partial w_0}{\partial x_2},\ \varepsilon_5^0 = \phi_1 + \frac{\partial w_0}{\partial x_1}$$

- The laminate constitutive relations are given as follows.

$$\begin{Bmatrix} \{N\} \\ \{M\} \end{Bmatrix} = \begin{bmatrix} [A][B] \\ [B][D] \end{bmatrix} \begin{Bmatrix} \{\varepsilon^0\} \\ \{\kappa\} \end{Bmatrix} \qquad (4)$$

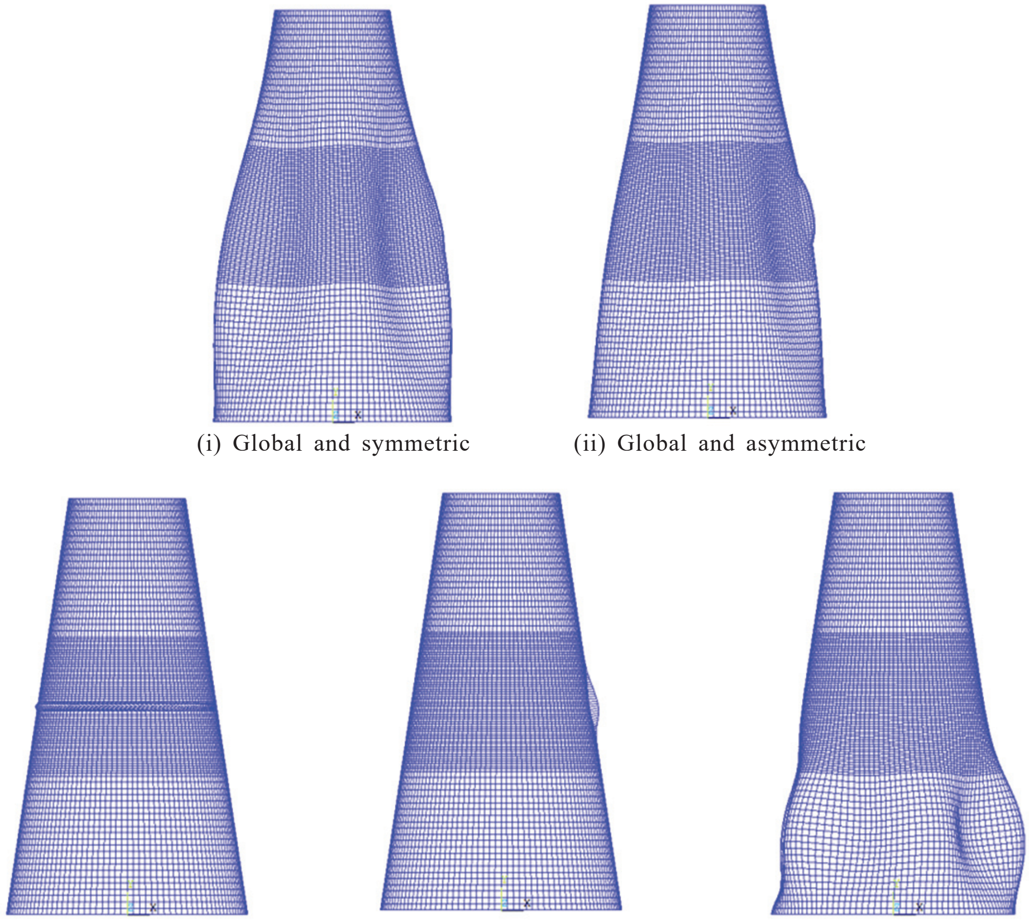

(i) Global and symmetric (ii) Global and asymmetric

(iii) Local and symmetric (iv) Local and asymmetric (v) Global mode beyond the delamination zone

Figure 4. Typical global and local buckling mode shapes in the conical shell under external pressure with embedded defect.

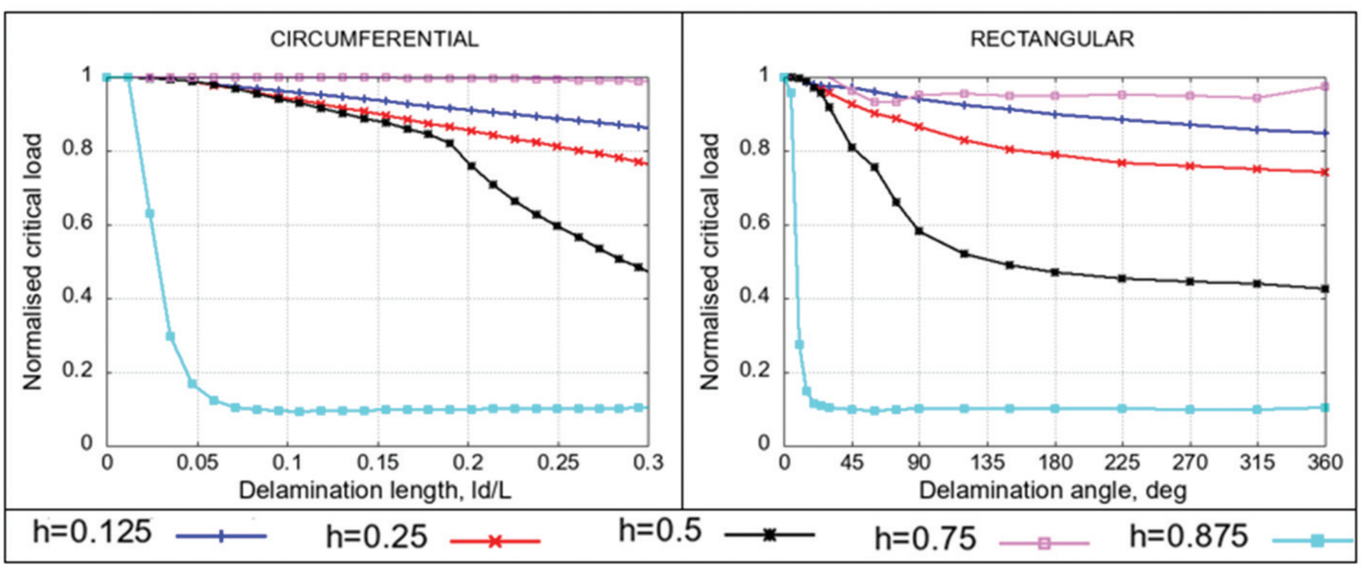

Figure 5. Effect of defect size on critical buckling pressure of isotropic conical shell.

$$\begin{Bmatrix} \{Q_2\} \\ \{Q_1\} \end{Bmatrix} = K_s \begin{bmatrix} A_{44} & A_{45} \\ A_{45} & A_{55} \end{bmatrix} \begin{Bmatrix} \varepsilon_4^0 \\ \varepsilon_5^0 \end{Bmatrix}$$

$$A_{ij} = \sum_{k=1}^{N} \bar{Q}_{ij}^k (\zeta_{k+1} - \zeta_k)\text{, for } i, j = 1, 2, 6$$

$$B_{ij} = \frac{1}{2}\sum_{k=1}^{N} \bar{Q}_{ij}^k (\zeta_{k+1}^2 - \zeta_k^2)\text{, for } i, j = 1, 2, 6$$

$$D_{ij} = \frac{1}{3}\sum_{k=1}^{N} \bar{Q}_{ij}^k (\zeta_{k+1}^3 - \zeta_k^3)\text{, for } i, j = 1, 2, 6$$

$$A_{ij} = \sum_{k=1}^{N} \bar{Q}_{ij}^k (\zeta_{k+1} - \zeta_k)\text{, for } i, j = 4, 5$$

- The equations of motion of simplified shell theory (in the coordinate system as shown in Fig. A.1) for a cross-ply laminated cylindrical shell of radius 'R' based on first-order shear deformation shell theory are as follows:

$$\frac{\partial N_1}{\partial x_1} + \frac{\partial N_6}{\partial x_2} = I_0\ddot{u}_0 + I_1\ddot{\phi}_1 \tag{5}$$

$$\frac{\partial N_6}{\partial x_1} + \frac{\partial N_2}{\partial x_2} + \frac{Q_2}{R} = I_0\ddot{u}_0 + I_1\ddot{\phi}_2$$

$$\frac{\partial M_1}{\partial x_1} + \frac{\partial M_6}{\partial x_2} - Q_1 = I_1\ddot{u}_0 + I_2\ddot{\phi}_1$$

$$\frac{\partial M_6}{\partial x_1} + \frac{\partial M_2}{\partial x_2} - Q_2 = I_1\ddot{v}_0 + I_2\ddot{\phi}_2$$

$$\frac{\partial Q_1}{\partial x_1} + \frac{\partial Q_2}{\partial x_2} - \frac{N_2}{R} - \hat{N}\frac{\partial^2 \omega_0}{\partial x_1^2} = I_0\ddot{\omega}_0$$

where, $I_i = \sum_{k=1}^{N}\int_{\zeta_{k+1}}^{\zeta_k} \rho^{(k)}\zeta^i d\zeta$ *for i = 0, 1, 2* are the mass inertia terms, N is the total number of layers, and $\rho^{(k)}$ is the material mass density of the k^{th} layer. The superposed dot indicates differentiation with respect to time.

REFERENCES

1. Sridharan, S. Delamination behavior of composites. Elsevier, 2008. 46 p
2. George, J.S. & Ziqi, Chen. Buckling of delaminated, long, cylindrical panels under pressure. *Computers & Structures*, 1988, **28**(2), 173–184.

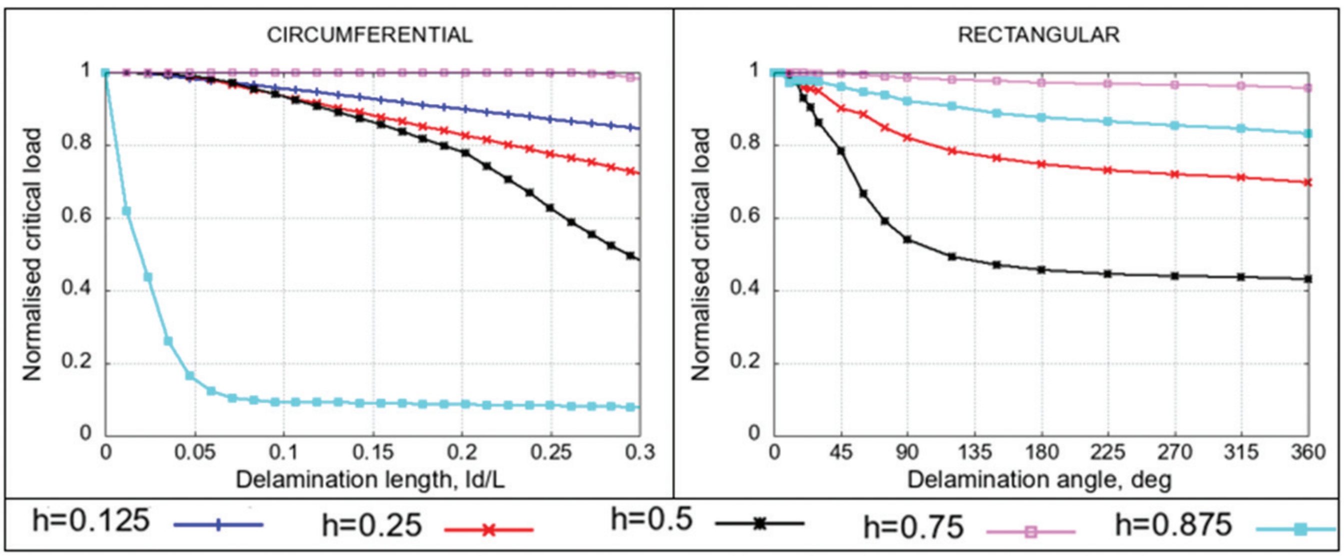

Figure 6. Effect of defect size on critical buckling pressure of composite shell (angle-ply).

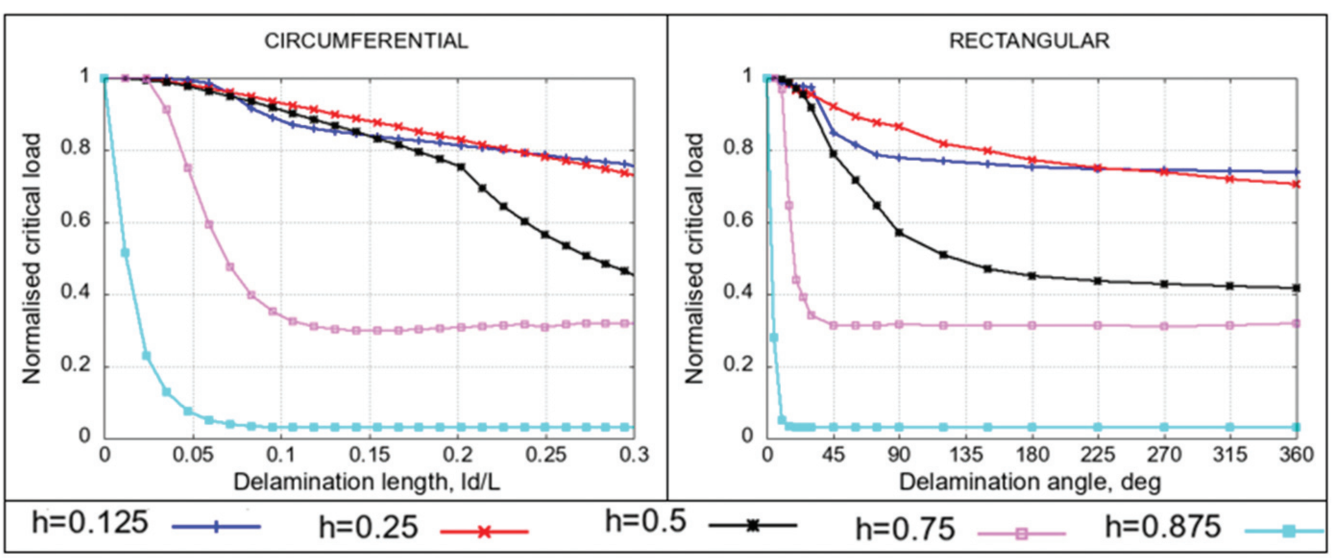

Figure 7. Effect of defect size on critical buckling pressure of composite shell (cross-ply0).

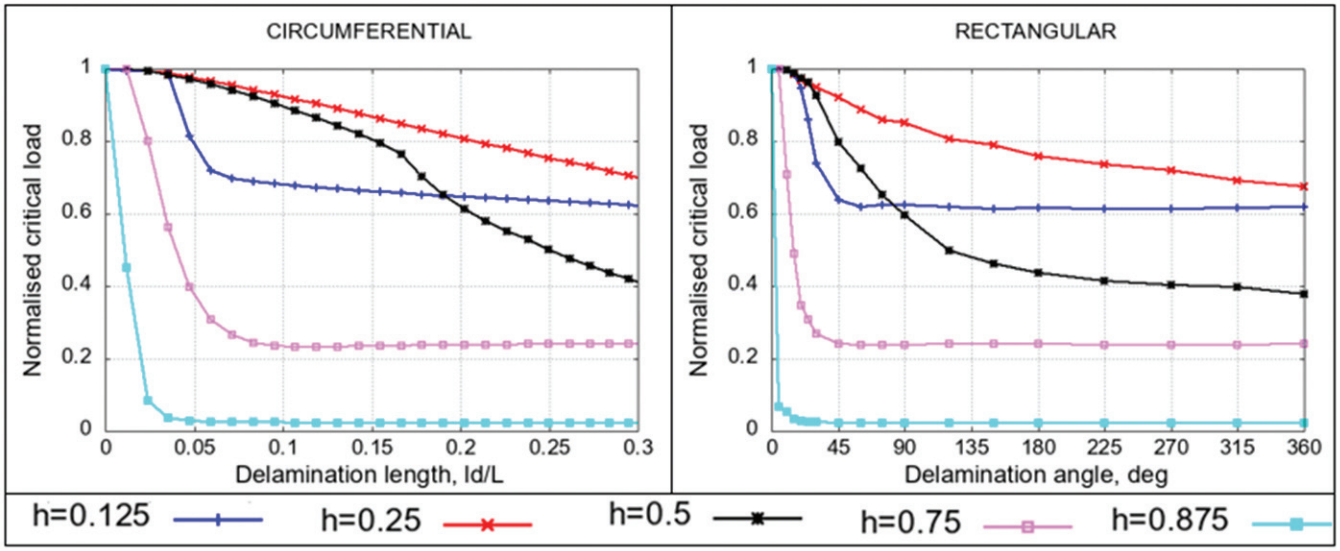

Figure 8. Effect of defect size on critical buckling pressure of composite shell (cross-ply90).

doi: 10.1016/0045-7949(88)90037-5

3. George, J.S.; Chen, Z.Q. & Sallam, S. Delamination buckling of cylindrical laminates. *Thin-Walled Structures*, 1991, **11**(1-2), 25–41.
doi: 10.1016/0263-8231(91)90009-8
4. Azam, Tafreshi. Delamination buckling and post-buckling in composite cylindrical shells under external pressure. *Thin-Walled Structures*, 2004, **42**(10), 1379-1404.
doi: 10.1016/j.tws.2004.05.008
5. Azam, Tafreshi. Delamination buckling and post-buckling in composite cylindrical shells under combined axial compression and external pressure. *Composite Structures*, 2006, **72**(4), 401-418.
doi: 10.1016/j.compstruct.2005.01.009
6. Jose, H.S.; Ameida, Jr.; Maikson, L.P.T.; Marcelo, L.R.; Volnei, Tita & Sandro, C.A. Buckling and post-buckling of filament wound composite tubes under axial compression: Linear, nonlinear, damage and experimental analyses. *Composites Part B*, 2018, **149**, 227-239.
doi: 10.1016/j.compositesb.2018.05.004
7. Zhenyu, Huang; Xudong, Qian; Zhoucheng, Su; Dinh, C.P.; & Narayanaswamy, Sridhar. Experimental investigation and damage simulation of large-scaled filament wound composite pipes. *Composites Part B*, 2020, **184**, 107639.
doi: 10.1016/j.compositesb.2019.107639
8. Behnam, Ameri; Morteza, Moradi; Bijan, Mohammadi & Davood, Salimi-Majd. Investigation of nonlinear post-buckling delamination in curved laminated composite panels via cohesive zone model. *Thin-Walled Structures*, 2020, **154**, 106797.
doi: 10.1016/j.tws.2020.106797
9. Das, K.; & Pandey, S. Effect of Delamination on static behaviour of point supported composite conoidal shells. Advances in structures, systems, and materials, *In* Lecture Notes on Multidisciplinary Industrial Engineering, Springer, Singapore, 2020, 51–63.
doi: 10.1007/978-981-15-3254-2_6
10. Baker, E.H.; Cappelli, A.P.; Kovalevsky, L. & Verette, R.M. Shell Analysis Manual, NASA CR-912, 1968, 610 p.
11. User Manual, Ansys Mechanical APDL 2019 R3.
12. Reddy, J.N. Mechanics of Laminated Plates and Shells: Theory and Analysis. CRC Press, New York, 2003. 449 p.

CONTRIBUTORS

Mr A. Nagendranath is a Scientist 'F' in DRDO-ASL, Hyderabad and a PhD scholar of Dept. of Applied Mechanics, IIT Madras. His areas of interest include: Design of composite structures, delamination, pressure vessels and Finite Element Analysis.
Contribution in the current study: Conceptualisation, numerical simulation and manuscript writing.

Dr Sanjay A. Khalane is a Scientist 'G' in DRDO-ASL, Hyderabad. His areas of interest include: Design of composite structures, FGM, stability of structures and vibration.
Contribution in the current study: Validation, resources, supervision.

Dr R.K. Gupta is a Distinguished Scientist (Retd.) and consultant at DRDO-ASL, Hyderabad. His areas of interest are: Aerospace structures, vibration, composites, aerospace system configuration design.
Contribution in the current study: Resources, supervision.

Dr C. Lakshmana Rao is a Professor in the Department of Applied Mechanics at Indian Institute of Technology (IIT), Madras. His research interests include modeling of failure of brittle materials, buckling control using smart materials and ballistic impact mechanics.
Contribution in the current study: Resources, supervision, review.